ISSN: 1687-1006 p
ISSN: 2682-3640 e

The Egyptian International Journal of Engineering Sciences and Technology

Vol. 39 (2022) 80–96

https://eijest.journals.ekb.eg/

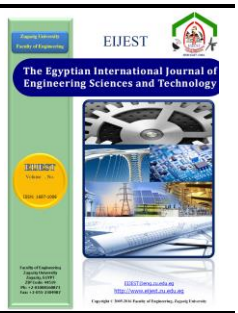

Reduction of Specific Absorption Rate: A Review Article

Alaa M. Hediya[a*], Ahmed M. Attiya[b], Walid S. El-Deeb[c]

[a] *Higher Institute of Engineering and Technology in Zagazig, Zagazig, Egypt.*
[b] *Microwave Engineering* Dept, *Electronics Research Institute (ERI), Cairo, Egypt.*
[c] *Electronics and Communications Engineering Dept Faculty of Engineering, Zagazig University Zagazig, Egypt.*

ARTICLEINFO

Keywords:

SAR reduction
Reflectors
RF-shields
Metamaterials
Hybrid method.

ABSTRACT

This paper presents a generic review of various methods performed to acquire a low SAR for antennas in different applications. While the SAR is minimized, various parameters such as bandwidth, gain, directivity, efficiency, and antenna size are also taken into consideration. However, it is not possible to achieve desirable results for all these parameters together. Thus, the SAR limitations include an imbalance between one or more of these parameters depending on the technique which is used to reduce the SAR.

Different techniques are used in SAR reduction like reflectors, designing a highly directive antenna, RF shielding using conductive and ferrite materials, RF shielding using Metamaterials such as AMC, DGS, SRR and EBG, or by using two or more methods simultaneously which is called hybrid method. Each of these types has its advantages and disadvantages that distinguish it from other types and determine the appropriate application for the use of this type.

This paper highlights most common SAR reduction techniques, and investigates the differences between them to make it easy for the researcher to select the proper type for each application. As well as, it presents a survey of the researches development of each methods during the past years and introduces a comparison between these researches from several aspects. A survey is also conducted for some recent research that achieves the required SAR value within MIMO systems. MIMO systems represent a key technology for 5G communications. Finally, a proposal was made for using hybrid method with MIMO antenna system to achieve low SAR with a highly performance.

1. Introduction

In conjunction with the great development of different industries, the need for antennas for multiple applications has increased. There is wide use of wireless body area networks (W-BAN) in different applications, e.g., mobile communications, medical diagnoses, military applications, or rescue services. In these kinds of applications, the antenna has a direct connection with the human body. The absorption of electromagnetic (EM) waves which travel in the free space may cause severe damages to the human tissues. Therefore, it is necessary to reduce the interaction of electromagnetic energy which is radiated towards the human body[1].

Specific absorption rate (SAR) is used to indicate the absorbed amount of EM waves by the human body. While minimizing the SAR, several precautions should be considered which are used in new antenna releases. These precautions include decreasing the size of the antenna, increasing the compactness of the antenna, increasing the robustness of the antenna,

*Corresponding author. Tel.: +201201573615
E-mail address: alaahediya@gmail.com

providing high-efficiency integration with the existing RF circuit components. These precautions vary depending on the application for which the antenna is being used[2].

Achieving the specified absorption rate (SAR) within the internationally allowed limit is one of the most important factors to be considered when designing the antenna. Thus, a survey study on this important research point is presented in this paper. First the internationally permitted SAR limits are discussed. Then, the main factors that affect the SAR value, and the different methods to reduce it are discussed in detail. At the end, a comparison is presented between several studies based on different methods.

2. Overview on SAR

2.1. SAR Exposure Limits

The local maximum SAR limits were set by IEEE (Institute of Electrical and Electronics Engineers) and ICNIRP (International Commission on Non-Ionizing Radiation Protection) in an uncontrolled environment. The ICNIR Recommendations are the most common in Europe. On the other hand, the standards set by IEEE which are slightly stricter and are applied in the United States. Australia and Japan have adopted the SAR limit as used in Europe 2 W/kg SAR for 10-g volume-averaged. SAR limits are defined at different time duration as shown in Table 1 [3].

2.2. Factors affecting the SAR

The SAR value is proportional to the square of the electric field which is absorbed into the human tissue. The SAR can be calculated as follows [4]:

$$SAR = \int_v \frac{\sigma(r)|\bar{E}(r)|^2}{\rho(r)} = c_t \frac{dT}{dt}\Big|_{t=0} \qquad (1)$$

Where, σ is the electrical conductivity of tissue, E is the electric field, ρ is the tissue mass density, c_t is the temperature of the tissue. The general form for the electric field in terms of the magnetic vector potential is given by [4]:

$$\bar{E} = \frac{1}{j\omega\mu\varepsilon}[k^2\bar{A} + \nabla(\nabla \cdot \bar{A})] \qquad (2)$$

where:

$$\bar{A} = \iiint_V \bar{J}\frac{e^{-jkR}}{4\pi R}\, dv' \qquad (3)$$

Where, ω is the angular velocity frequency, μ is the permeability, ε is the complex permittivity, $k=\omega\sqrt{\mu\varepsilon}$ is the vector wave number, $\bar{A}$ is the magnetic vector potential, $\bar{J}$ is the electric current density, and R is the distance from the source to the field point. Thus, it is clear that the current distribution formed on the antenna affects the electric field as well as the SAR value. Thus, by increasing the current uniformity, the current intensity is increasing and the SAR can be reduced without affecting the far field performance [4].

Table 1. SAR limits [3].

Region	USA	Europe	Australia	Japan
Organization/ Body	IEEE/ANSI/ FCC	ICNIRP	ASA	TTC/MPTC
Measurement method	C95.1	EN50360	ARPANSA	ARIB
Whole-body averaged SAR	0.08 W/kg	0.08 W/kg	0.08 W/kg	0.04 W/kg
Spatial-peak SAR in head	1.6 W/kg	2 W/kg	2 W/kg	2 W/kg
Averaging mass in head	1 g	10 g	10 g	10 g
Spatial-peak SAR in limbs	4 W/kg	4 W/kg	4 W/kg	4 W/kg
Averaging mass in limbs	10 g	10 g	10 g	10 g
Averaging time	30 min	6 min	6 min	6 min

It should also be taken into account that the value of SAR is affected also by a set of other parameters like the operating frequency, the polarization and the configuration of the antenna. The values of these parameters can be controlled by adjusting the antenna design in various ways to reduce the SAR to acceptable values while maintaining the other characteristics of the antenna with acceptable values [5].

2.3. Calculation of SAR reduction

To reduce the specific absorption rate, the value of the electromagnetic waves that flow toward the human body tissue must be reduced. This can be done either by changing the design of the antenna itself, or by placing an additional element with the antenna to absorb unwanted radiations. It can also be obtained by distracting these unwanted radiations. These changings should preserve the original characteristics of the antenna and, if possible, improve them. Whatever the modification method is used, the

efficiency and appropriateness of the new antenna modulation in a reduction of the SAR values are calculated by comparing the modulus value before and after the modification. To calculate the SAR reduction in a more quantitative way, a new parameter; Specific Reduction Factor (SRF); is defined as follows [6].

$$SRF_{1_g}(\%) = \frac{SAR_{1g} - SAR_{1g,after}}{SAR_{1g}} \times 100 \qquad (4)$$

$$SRF_{10_g}(\%) = \frac{SAR_{10g} - SAR_{10g,after}}{SAR_{10g}} \times 100 \qquad (5)$$

Where SRF_{1g} is the SAR reduction factor for 1g peak SAR, SAR_{1g} is 1g peak specific absorption rate before modification, $SAR_{1g,after}$ is the 1g peak specific absorption rate after modification, SRF_{10g} is the SAR reduction factor for 10g peak SAR, SAR_{10g} is 10g peak specific absorption rate before modification, $SAR_{10g,after}$ is the 10g peak specific absorption rate after modification. It should be noted that the effect of the SAR reduction increases with the increase of the value of SRF.

3. Methods of SAR Reduction

3.1. Reflectors

By using the reflector integrated with the main antenna, it is possible to improve the effective efficiency. It can also be used to reduce the SAR value. The reflector is placed between the main antenna and the human head. Thus, it reduces the radiation toward the human head (which reduces the SAR). It also increases the radiation pattern in the opposite direction (which increases the antenna gain). Fig.1 shows a typical arrangement of reflectors with conventional monopole antenna and human head model [7]. Haridim. used two rode reflectors with traditional monopole antenna to achieve SAR reduction of 7.5 dB (42.17 %) or more, with minimum distortion of the required radiation pattern[7].

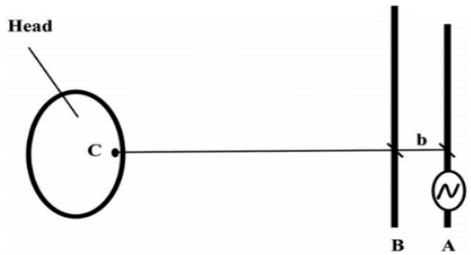

Fig. 1. Reducing the SAR effect by using a reflector [7].

However, using reflectors has many disadvantages. The most prominent disadvantage is increasing the antenna size significantly [7]. This defect was addressed in some other researches by making the reflector element compactable with the antenna in the same substrate which showed relatively acceptable results. Atanasov et al. [8] combined a conventional monopole antenna with a compactable reflector built on the same substrate. In this case, they could improve the performance of the antenna and achieve an averaged SAR of 0.0971 W/Kg [8]. M. El Atrash et al. [9] surrounded a mender line antenna by a compactable U-shaped reflector. This configuration was found also to be suitable for SAR reduction.

There is also another disadvantage for using this method. Reducing the SAR in the direction of the reflector can affect the shape of the radiation pattern. This results in the presence null regions. The signal would be lost if it is required to use one of these null regions. Reflector may also increase the SAR values in case of an incorrect direction by the user during the operation of the antenna. Hence one of the limitations in using this method is to obtain high efficiency and not to influence the radiation pattern. In addition, it is also required to maintain as much as possible the appropriate size of the antenna at low cost. The total cost increases due to the addition of the reflector element.

Another technique was developed by using more than one antenna element like a phased array antenna instead of using an antenna with a reflector. The radiation pattern in the phased array antenna is distinguished by the fact that it cancels radiation in the near field region without affecting the radiation pattern of the far-field region. Even further its use improves efficiency compared to the single element antenna. However, the aforementioned problem of increasing the size and cost of the antenna remains in this method too. Moreover, this method was not used for a several years ago due to the presence of better alternatives in terms of efficiency, size and cost. Mangoud et al. [10] used phased array antenna. The specific absorption rate was reduced by more than 10 dB, in conjunction with improved efficiency compared to the conventional antenna.

3.2. Highly directive antennas

The use of a high-directional antennas is one of the methods which can be used to reduce the SAR. This method depends on reducing radiation in all directions except for the main lobe direction of the antenna radiation. Thus, the radiation on the human body can be reduced when the main beam is adjusted in a direction opposite to the direction of the human body. The problem with this method is that it leads to the degradation of the received signal in all other

directions except for the direction of the main lobe. Thus, this method is not common, especially in the field of mobile phones. However, it can be used in some special applications.

Laila et al. [11] discussed a design of a modified CPW fed monopole antenna. This antenna is considered as highly directive antenna. The SAR of this antenna is reduced by 20 % by reducing radiated power in one quadrant of the radiation pattern. The antenna was placed such that this quadrant of the radiation was facing the human body tissue [9]. Choi et al. [4] used PIFA antenna to introduce 11 % improvement in the SAR reduction value while the antenna efficiency is improved by 2.6 dB. On the other hand, Bhattacharjee et al. [10] used a modified T-shape antenna to introduce 25.19 % reduction on SAR while the efficiency is increased to 96.9 %.

3.3. RF shielding for SAR reduction

Electromagnetic shielding is defined as reducing the electromagnetic field in a specific area by blocking the field by using an obstacle made of conductive or magnetic materials. When the electromagnetic shielding blocks radio frequency (RF) electromagnetic radiation, it is known as RF shielding. The amount of reduction of the electromagnetic field depends on the frequency, the used material for shielding, the thickness of shielding material, the size of the shielded tissue, the direction of the holes in the shielding surface, and their shape and size. RF shielding is commonly based on electric or magnetic conductive material like copper. Artificial negative refractive index metamaterials are also found to be suitable for electromagnetic shielding [11].

3.3.1 Conductive, ferrite, and dielectric shielding

The radio frequency (RF) shielding materials include natural materials like conductive materials, ferrite materials and lossy dielectric materials. The properties of the conductive and lossy dielectric materials dependent on conductivity, relative permittivity and mass density. Examples of conductive materials are copper, and aluminum. On the other hand, lossy dielectric materials include silicon, graphite, and carbon black. Ferrite materials have both electric and magnetic absorption. Ferrites are produced by mixing the iron oxide with other metal oxides. Table 2 shows the properties of a group of conductive and dielectric materials which can be effective for RF Shielding [12]. Table 3 shows the properties of a ferrite which can be used for RF shielding [12].

The RF shielding absorbs electromagnetic radiations. The charge carriers are affected by the force produced by the electric field. If an ideal conducting surface is exposed to electric field, an induced current is formed which leads to displacement of charges inside the conductor. Therefore, the current distribution on the conductor surface is canceled. Similarly, the magnetic fields introduce eddy currents which are formed as a result of time variation of these magnetic fields [13, 14].

Ultimately, electromagnetic radiation is reflected from the conductor surface. The drawback of this method is that the exciting field does not completely cancel the incident field. This is because of the electrical resistance of the conductor. This property has a significant effect at low frequencies. Thus, the ferromagnetic response of most conductors increases when decreasing the frequencies of the magnetic field. As a result, such fields are not fully weakened by the conductor. However, this method is somewhat effective in the case of high frequencies. If the shield is very thin, this leads to a complete absorption of radiation within the skin depth [13, 14].

Chan et al. [17] placed RF Shield on the different types of mobile phone surface as shown in Fig.2 in an attempt to reduce SAR. They checked several shapes and sizes of aluminum shields to introduce SAR reduction of 20 % [15]. Hanafi et al. [18] studied numerically the effect of aluminum shield when placed on mobile model surface as shown in Fig.3 They obtained SAR reduction of 26.4 % [16]. Rani et al. [19] tried to reduce SAR of the traditional dipole antenna by using several types of shielding materials of differing shapes and sizes as shown in Fig.4. They studied the effect of several conductive materials such as Aluminum, Copper, Nickel, Silver, Zinc. They could obtain SAR around 88 % for all types of materials. In this case, it is found that the best material for SAR reduction by using RF shielding is Nickel, which reduced the SAR value by 97.7 % [17]. Dutta et al. [20] studied the effect of the SAR generated by the traditional inverted F antenna placed inside the mobile phone, which is shown in Fig.5-(a) on a spherical model that simulates the human head. The antenna had a SAR value of 1.1 W/Kg in the absence of RF shield. Then, they studied the effectiveness of RF Shields that is placed on the mobile phone cover as shown in Fig.5-(b) in reducing SAR. They used several shielding materials including Copper, Aluminum, Teflon, and Germanium. The best of all is the germanium shielding, which reduced the SAR of the brain to 0.08 W/Kg [18]. Ragha et al. [21] studied the effect of the change in the shape and size of the RF shielding on the value of the SAR. They used several forms of RF shields of ferrite material placed on the outer surface of the mobile phone model close to a cubic model

which simulates a human head. They could reduce the SAR by a factor 56.74 % [19]. They also studied the effect of several designs of RF shielding as shown in Fig.6 on SAR reduction by using conventional dipole antenna, and spherical head model. They reduced the SAR by a factor 82.25 % [20].

Conductive or ferrite shielding are placed on the outer surface of mobile phones towards the human head. In this case the shielding is used as a reflector. They also have similar advantages of reflectors where they reflect electromagnetic waves from the side of the human head to the opposite direction. Lossy insulating shielding materials have a similar technique. However, the main difference in these cases these materials absorb electromagnetic waves instead of reflecting them. Thus, these shielding materials introduce large loss and less gain. This is an uncommon method [12]. Hossain et al. could reduce the SAR by 40 % by using a double layer of copper and silicon [21].

The new trend in RF shielding for SAR reduction is using metamaterial. Thus, the use of conducting, ferrite, and lossy dielectric materials has decreased significantly in this application. Table 4 shows a comparison between different RF shielding techniques.

3.3.2 Metamaterials Shielding

Metamaterials are synthesized materials having special properties which are not available in natural materials. They are usually made from multiple elements fashioned from composite materials like metals and dielectrics. Metamaterial can manipulate electromagnetic waves by blocking, bending, enhancing, or absorbing waves, to achieve benefits which are not available in conventional materials [22]. Fig.7 shows the mechanism of EMW refraction by using metamaterial as an example of metamaterial usages [23]. The properties of the metamaterials depend on their ergonomically designed structures, the precise shape, size, orientation, geometry, and arrangement, regardless of the base materials. The basic requirement for metamaterials is that their elementary units should be much smaller than the operating wavelength. These materials are also defined as negative-index material where the value of the refraction index of it is negative [24, 25]. Each metamaterial structure has a range of operating frequency [26]. Properties of metamaterial are determined by studying their corresponding dispersion diagrams including their pass bands and stop bands [27, 28].

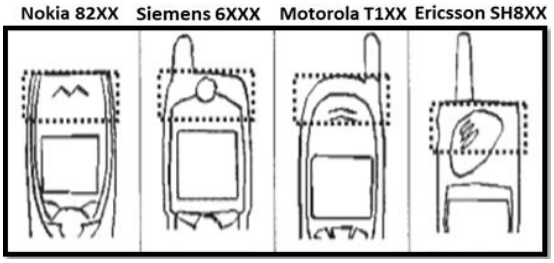

Fig. 2. The position of the aluminium RF-shield relative to different types of mobile phone [14].

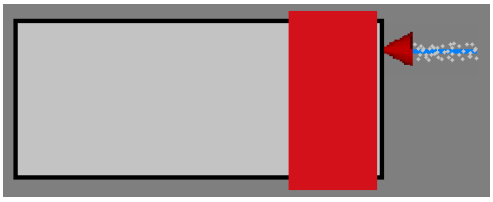

Fig. 3. The position of aluminium RF-shield relative to mobile phone model [16].

Table 2. Properties of different materials[12].

Material	σ	εr/μr
PEC	∞	1
Copper	5.8e7	1
Aluminum	3.8e7	1
Silicon	4.4e−4	11.9
Graphite	9.24	1.52
Carbon	7.56	1.95

Table 3. Properties of different ferrite materials [12].

Material	σ (S/m)	εr	μr	δe	ρ (kg/m3)
Ferrite sheet	4	7	2.8	–	5270
BaFe12O19	–	24	2	1e−6	–

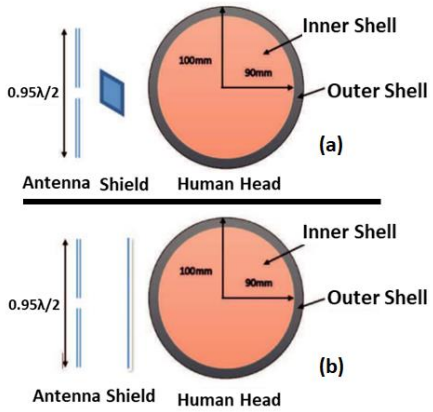

Fig. 4. The use of different dimensions and positions of RF-shields [17].

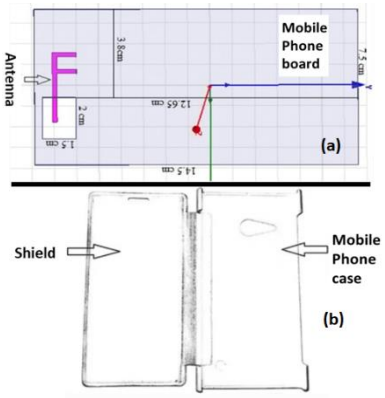

Fig. 5. The use of conductive sheet with PIFA antenna [18].

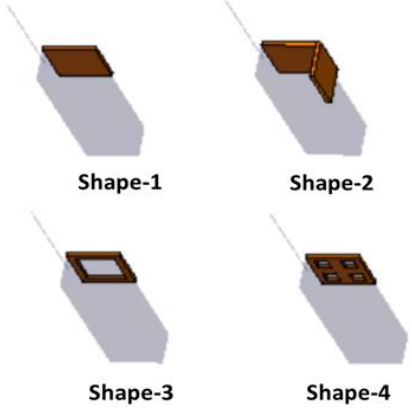

Fig. 6. The use of different shapes of conductive sheets with mobile phone model [20].

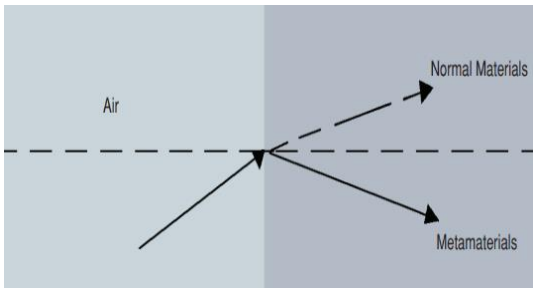

Fig. 7. Light bends the "opposite way" when it enters from the vacuum to the metamaterials [23].

3.3.2.1 Metamaterials Based on Split-Ring Resonators

Microwave frequency metamaterials are commonly constructed as arrays of electrically conductive loops of wire that have suitable capacitive, and inductive characteristics. These metamaterials are known as split-ring resonator metamaterial [29]. The configuration is one of the most common methods used to synthesize double negative metamaterials. A single cell SRR consists of a pair of enclosed loops whether circular, square, or other loop shapes, made of metal like copper with splits in them at opposite ends [30]. In this case the magnetic flux permeates the metal ring, thus a rotating current is induced inside the rings producing an induced flux which opposes the incident field. The small gaps between the rings control the capacitance values which in turn controls the resonating frequency. The dimensions of the structure should be smaller than resonant wavelength that's being millimeters when dealing with microwave frequency radiations. This will lead to low-radiative losses, and high-quality factors [31]. Each cell of SRR sheets can be designed to have its own electromagnetic response. Some examples of SRR are shown in Fig.8 and Fig.9 [32]. The response can be boosted or lesseed by appropriate design of such SRR. SRRs are distinguished from ferromagnetic materials because they are more active, lighter, and can be more effective at lower power [33]. There are many types of split-ring resonators such as; the 1-D split-ring structure, the Omega structure, the symmetrical-ring structure, the two-layer multi spiral resonator (TL-MSR), the open split-ring resonator (OSRR), the broadside coupled split-ring resonator (BC-SRR), etc [34].

Several examples of SRR have been used in reducing SAR. Rosaline et al. placed traditional SRR superstrate for a traditional rectangle patch antenna as shown in Fig.10 towards a 6-layer head model. They could reduce the SAR by 86 % [35]. Rosaline et al. added a partial split ring in addition to pair of symmetrical stubs, to a circular monopole antenna. Through this configuration, they were able to enhance the bandwidth and reduce the SAR by 12 % [36]. Zhou et al. added three integrated SRRs shown in Fig.11 on a smart plastic case to a mobile phone handset. They could reduce the SAR from 2.49 W/Kg to 1.78 W/Kg by 30 % [37]. Messaoudi et al. added three traditional SRRs to the dipole antenna integrally on the same chip to reduce SAR by 84.3 %. They also integrated one SRR with PIFA antenna to reduce SAR by 23.7 % [38]. Saraswat et al. achieved SAR reduction by about 13.3 % for a new planner antenna design supports multiband, using two types of metamaterials a slotted circular shape, and a complementary-SRR. In addition, they used T-shaped slots instead of a homogenous ground plane to improve antenna performance [39]. Tamim et al. integrated SRRs and a new design of double-inversed E shaped structure resonator that shown in Fig.12 with mobile a phone antenna to reduce the SAR on a SAM phantom head model by 44 % [40]. Rosaline et al.used a slab of metamaterial of SRR in a rectangular patch antenna. This artificial slab consists of an array of pentagon split ring resonator. The result of this antenna configuration showed a reduction of SAR by 84.5 % while improving efficiency [41]. Ganeshwaran et al.

used hybrid SRRs consists of one circular ring inside two square rings constructed on separated substrate and placed behind a mender line patch antenna to achieve SAR value of 0.651 W/Kg over 1g tissue [42]. Ramachandran et al. used (2×3) array of hybrid SRR with a mobile phone model to reduce SAR value up to 36.646 % [43]. Table 5 shows a comparison between different SRR techniques.

3.3.2.2 Metamaterials Based on Electromagnetic Band Gap

Electromagnetic band gab (EBG) structure is an artificial periodic structures that avert electromagnetic waves or assist the propagation of them only in a specified band of frequencies for all polarization states and all incident angles, due to the periodic variation in the refractive index inside it [44]. This variation produces forward and backward propagating waves that affect each other through the coupled wave equations. EBG led to the strategy to have a complete control over electromagnetic waves by solving coupled wave equations. The dispersion relation it was found that; there was no wave propagation along with a certain frequency band due to the evanescent waves. The EBG structure is similar in composition to a group of cavities and waveguides which are widely used to control the propagation of microwaves[1]. Metallic cavity prevents microwaves to propagate under a certain threshold frequency, and conducting hollow waveguide allows wave propagation along its axis only [45]. The periodic EBG structure may be formed on a substrate, or on the ground plane. They may be realized by drilling, etching, and cuffing on the metal or dielectric substrates [46]. EBG is capable of blocking electromagnetic propagation in all selected directions. EBG may be 3-D, 2-D, or 1-D crystals. In the case of dealing with the compact antennas, it is preferable to deal with the 1-D EBG crystals to maintain a small size of the antenna as shown in Fig.13 [47].

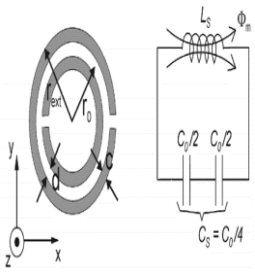

Fig. 8. SRR equivalent-circuit model [32].

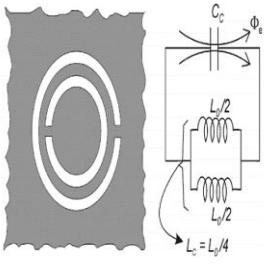

Fig. 9. CSRR equivalent-circuit model [32].

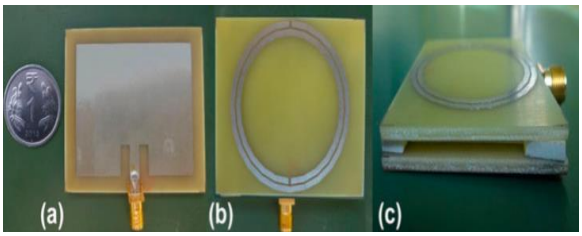

Fig. 10. The fabricated prototype (a) conventional patch antenna (b) antenna along with SRR superstrate (top view) (c) antenna along with SRR superstrate (side view) [35].

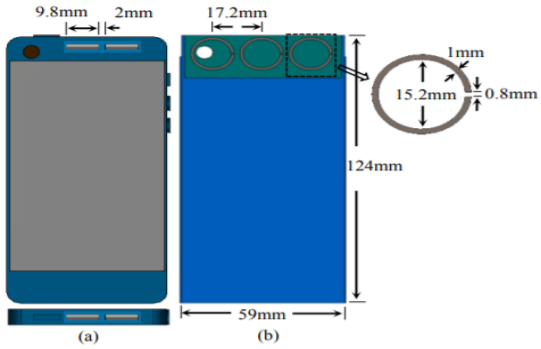

Fig. 11. (a) The Wi-Fi dipole antenna placement in a cellular phone (back and side view). (b) The proposed SRR phone [37].

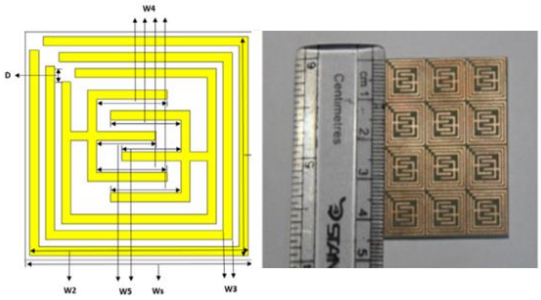

(a) (b)

Fig. 12. (a) The configuration of SRR unit cell. (b) The prototype of 3×4 SRR array [40].

On the other hand, the electromagnetic bandgap (EBG) structure is considered one of the most important designs which can be used to improve the antenna efficiency while maintaining its bandwidth [48]. Ikeuchi et al. studied the effect of the EBG substrate on reducing SAR, and comparing it with the PEC substrate. A dipole antenna operating at a frequency of 3.5 GHz for 4G mobile communication was investigated in this case. Using PEC substrate with the traditional dipole antenna introduces an antenna efficiency reaches to 82 % and also the SAR value is reduced to (14 - 36) %. On the other hand, using EBG substrate increases the efficiency increased to 91 % and the SAR is decreased by a ratio 84 % In

the design shown in Fig.14 [49]. Khan et al. integrated EBG structure with new design of planner dipole antenna for wearable applications. They were able to reduce SAR by 98 % while increasing gain by 9 dB. The return loss is also improved to be 28 dB [50]. Ali et al. added an EBG to a traditional microstrip antenna to achieve a peak SAR value of 1.79 W/Kg, which has been reduced by 10.5 %, while improve efficiency from 55.51 % to 74.04 % [51]. The EBG method is preferred compared with SRR method due to the large variety of the resonant and cross-polarization effects when using the SRR method. Therefore, the EBG method has become more common in SAR reduction [52].

Tharakan et al. placed 4×6 EBG array structure near a dipole antenna to reduce SAR on a 6-layer head model from 48.1 W/Kg for the dipole in free space to 1.46 W/Kg, by a reduction factor 97.92 %. They applies this method also for PIFA antenna inside a mobile board [53]. Umar et al. placed a group of EBG cells around a square patch antenna as shown in Fig.15 from all directions. By using this method they reduced the SAR value by 77.9 % [54]. Ashyap et al. integrated a novel design of miniaturized EBG structures to a compact wearable antenna as shown in Fig.16 to achieve reduction on SAR by 95 % [55]. Manikonda et al. added a novel E-shaped EBG array chip, to a textile patch antenna, as shown in Fig.17 for reducing SAR from 1.49 W/Kg to 0.76 W/Kg, by a reduction factor 48.99 % [56]. Balakrishnan et al. placed a chip containing a novel design of EBG structure between the chip that contains T-shaped folded dipole antenna and the human head model to reduce the SAR of the antenna by 99 % [57]. El Atrash et al. added 3×3 EBG cross-shape elements shown in Fig.18 between the head model and an oval-shaped monopole antenna shown in Fig.19 to reduce SAR by 99.5 % [58]. Pei et al. used a textile EBG ground plane, with an innovative-belt antenna, to reduce SAR by up to 98.52 % (from 2.71 W/Kg to 0.04 W/Kg) [59]. (S. Singh et al, 2021) were able to reduce SAR by more than 90 % while improve efficiency, by using 3×3 array of hexagonal-shaped EBG between the head model and the compact wideband stub loaded monopole antenna (CWSLMA) [60]. El May et al. applied (2×2) rectangular EBG array with slots to a monopole antenna with a rectangular patches to reduce SAR value more than 95 % [61]. Wissem et al. integrated (4×3) EBG array with textil microstrip antenna to reduce SAR value more than 69.9 % [62]. Table 6 shows a comparison between different EBG techniques.

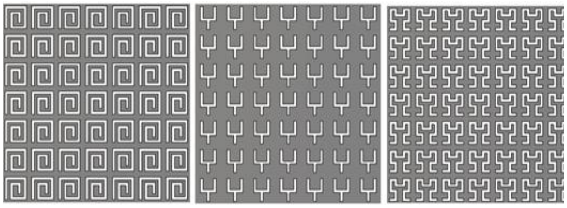

(a) (b) (c)

Fig. 13. Front view of the Array of EBG structure. (a)spiral (b)fork (c)fractal [47].

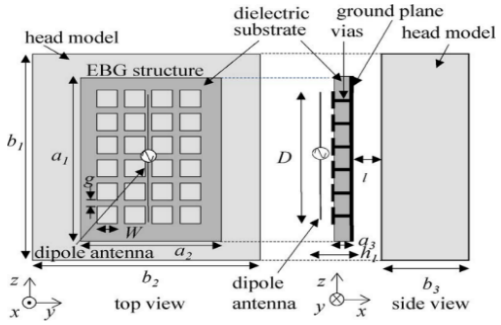

Fig. 14. Geometry of the antenna with the EBG substrate and cubic head model [49].

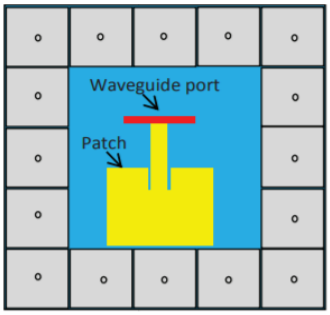

Fig. 15. The layout of patch antenna with a mushroom EBG ground plane [54].

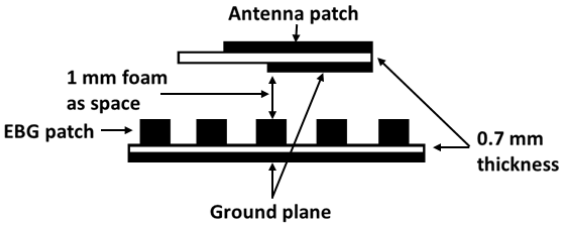

Fig. 16. The geometry of the patched antenna with EBG array shield [55].

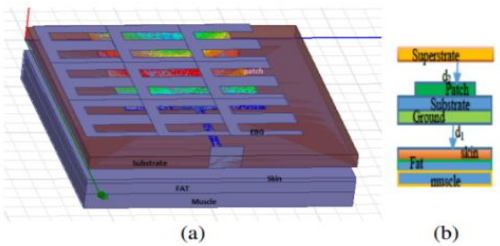

Fig. 17. The E-shape antenna with EBG array (a) front view (b) side view [56].

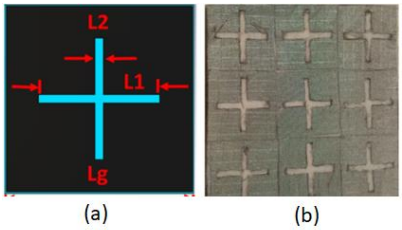

Fig. 18. (a) The geometry of EBG unit cell. (b) The prototype of EBG array [58].

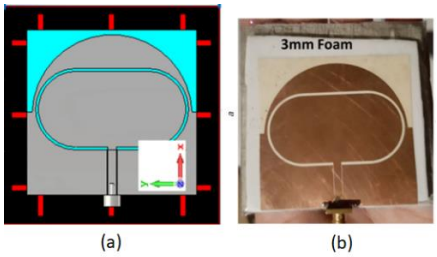

Fig. 19. The wearable patched antenna with an EBG shield (a) design (b) prototype [58].

3.4 Hybrid method

Recently most studies of the SAR reduction do not use only one of the above methods. Thus, a new trend has emerged where more than one of these methods are integrated together to obtain the best possible results in terms of SAR reduction. In addition, these combined methods do not have an undesirable effect on antenna performance, while reducing the SAR. In the hybrid method we can also add two shields to the antenna one to improve its performance and another part to reduce the SAR value. The challenge here is to achieve the desired results with the least size and cost possible.

Chan used a hybrid of phased array antenna and EBG substrate. Thus, the reflector method and the RF shielding method were combined together to achieve efficiency over 94.3 % and reduction on SAR over 70 %. The proposed configuration is shown in Fig.20 [63]. Rosaline used SRR technology with a compact directional microstrip antenna to reduce the average SAR by a factor 93 % , with 63 % impedance matching and 28 % size miniaturization [64]. Ashyap et al. used two metamaterials EBG and FSS with fabric CPW antenna for wearable application. They could reduce the SAR by a factor 95 %. At the same time they were improved the gain to 6.55 dBi [65]. Gao et al. used a directive PIFA antenna with EBG array chip to improve the gain from -0.6 dBi to 4.5 dBi. They studied the relationship between the number of EBG units to the decrease the SAR value. They could reduce the SAR by a factor 98.74 % [66]. Ashyap et al. used both EBG and Defected Ground Structure (DGS) with wearable symmetric E-slot antenna as shown in Fig.21. The use of DGS led to improve the gain by 6.45 dBi , and the use of EBG chip led to reduce the SAR by more than 90 % [67]. Hazarika et al. improved the gain of two compact monopole antenna by 85 %, comparable to simple monopole, using DGS. At the same time they could decrease the SAR by a factor 99.5 % by using Artificial Magnetic Structure (AMC) [68]. Alhawari et al. used 6-elements of metamaterial with a planner textile antenna each element consists of novel defected structure shape within SRR to achieve SAR value less than 2 W/Kg and band width from 6.5 GHz to 35 GHz [69]. Reo et al. placed a plate consist of two EBG arrays and two SRR arrays behind the S-shaped antenna to achieve SAR value of 0.944 W/Kg [70]. Table 7 shows a comparison between some hybrid techniques examples.

4. Comparative Studies

In the Table 8 a detailed comparison was made for a group of studies that were previously mentioned in this paper in terms of antenna parameters that determined antenna performance and application. In the Table 9 the same references had been used to compare them in terms of SAR reduction. The studies were chosen to include all the methods of reducing SAR that were mentioned. To show the best methods used as well as to show the evolution of SAR reduction techniques over the years from 1999 until today.

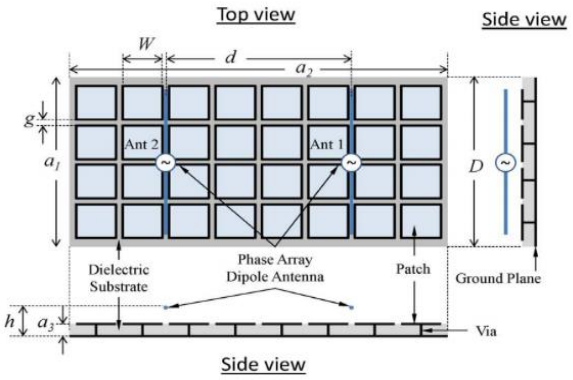

Fig. 20. Geometry of the dipole phased-array antenna above an EBG substrate [63].

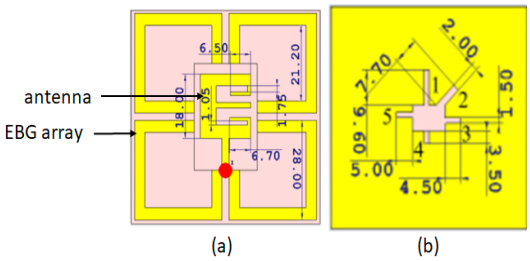

Fig. 21. The integrated antenna with EBG-DGS (a) front view (b) bach view [67].

5. Future scope

In the few past decades, the wireless communication has evolved greatly for all applications, and the fifth generation (5G) communications appeared. This led to a major development economic and social field. Thus, the trend towards 5G communications is still increasing [71, 72]. The key technique of 5G communication is Multiple-Input-Multiple-Output (MIMO) wireless systems technique. The main features of this technique are channel capacity enhancement and communication performance improvement without providing additional bandwidth (BW) or increasing power at the source. These features are achieved through, presence of multiple antenna elements in both transmitter and receiver [73]. However, using MIMO antennas require several requirements like, small size, high performance, low mutual coupling. In this case low SAR would be more complex compared with single antenna [74].

The difficulty in achieving a low SAR value less than the permissible limit; 2 W/Kg; is that the SAR value in the case of the MIMO system is the sum of the SAR of the antennas. Therefore, it is necessary to reduce the SAR value of the individual antenna very much less than the permissible limit. Several of previous methods are applied to reduce the SAR value and at the same time ensure the performance of the MIMO systems. There are a few studies have dealt with SAR accounts in addition to MIMO coefficients, due to the difficulty of achieving them.

Achieving a good SAR coefficient for MIMO system operating in 5G for wireless communications remains one of the most important demands which should be taken into consideration.

Tu et al. added a DS-EBG structure to an 8-element MIMO antenna to improve MIMO characteristics like gain, and mutual coupling. This is obtained by improving the resulting radiation resistance, and the radiated power. They obtained a total SAR value for 8-element antennas less than 1.19 W/Kg [75]. Jiang et al. designed an 8-element Folded monopole MIMO antenna for 5G smartphone communications. They could obtain a total SAR value <1 W/Kg by using grounding branch technique [76]. Serghiou et al. designed an 8-element MIMO antenna by using full ground structure acts as RF-shield. They could reduce the SAR value of some antennas inside the MIMO system to 0.12 W/Kg [77]. Sugumaran et al. added FSS and EBG shield to a 4-element textile MIMO system, where the individual element is a compact monopole antenna. They could obtain antenna efficiency of 80.12 % with an average SAR factor less than 0.2 W/Kg [22]. Gupta et al. designed two element MIMO antenna system using monopole antenna with L-shaped partial ground plane and U-shaped stubs to reduce the mutual coupling and the SAR value. This MIMO system has a total SAR value of 0.511 W/Kg over 1g of tissue [78]. Zu et al. added a (17×7) uniplanar compact EBG array on distance 4 mm from the ground surface of a 4-element MIMO antenna to achieve SAR value of 0.59 W/Kg [79].

Based on the previously mentioned SAR reduction methods, we used a (5×4) DGS arrays on both sides of each element of MIMO during BW from (3-5) GHz. The antennas of this MIMO system achieved coupling coefficients less than -15 dB and total SAR value for all system antennas that does not exceed 2W/Kg over 1g tissue at the resonant frequency and several other frequencies within the antenna BW [80].

We also look forward in the future to using the hybrid method in our design by applying additional SAR reduction method simultaneously with DGS on a separated substrate behind the ground plane of the system to reach the best possible results. Table 10 shows a comparison between the proposed MIMO system and several recent related works mentioned in this section.

antenna system consisting of six folded dipole antennas to achieve low SAR, and low mutual coupling

6. Conclusion

Specific Absorption Rate (SAR) is one of the most important factors which should be into consideration when designing antennas for portable communication system. due to the great damage caused by absorbing harmful electromagnetic waves in the human body. Especially when designing antennas that exposed directly to the human body, such as mobile phone antennas or wearable antennas. There are many parameters by controlling it, the SAR value can be reduced such as position, size, and thickness of antennas. In this paper, we discussed the SAR problem, we also presented the factors affecting it and how to calculate its value. We also conducted a survey about many effective methods for reducing SAR. The RF-Shields are the most effective method, especially using metamaterial substrate. The RF-Shields are the most effective method, especially using the EBG substrate. But when using one of these methods to reduce SAR value, consideration must be taken to maintaining other important factors affecting the operation of the antenna, such as impedance matching, provides high efficiency, decrease the size of the antenna, increase compactness and robustness of antenna, and integration with the existing RF circuit components.

Table 4. Comparison of Different Shielding Techniques.

Reference	SAR source (Antenna)	Resonant frequency	Antenna size	RF-Shield material	RF-shield size	Material classification	Reduction on SAR (%)
[15] 2005	Mobile phone (Nokia 62, Siemens 8, etc.)	(900 and 1800) MHz	NA	Aluminum	(5×2) cm^2	Conductive material	20
[16] 2011	Numerically calculation	900 MHz	Mobile phone model box (40×100×18) mm^3	Aluminum	(20×70×t) mm^3, t= (1, 2, or 3) mm		26.4
[17] 2015	Dipole antenna	900 MHz	0.95(λ/2) dipole	Nickel	(2×2×t) mm^3, t= (0.1, 0.2. or 0.3) mm		97.7
[18] 2016	Mobile phone with PIFA antenna	1800 MHz	PIFA antenna on mobile board (145×75×10) mm^3	Germanium	(145×75×t) mm^3, t= (1, or 2) mm		92.7
[19] 2009	Mobile phone	2.4 GHz	NA	Ferrite material	various types and sizes	Ferrite material	56.74
[20] 2009	Dipole antenna	900 MHz	(λ/2) dipole	Ferrite material	various types and sizes		82.25
[21] 2015	Mobile phone with PIFA antenna	(900 and 1800) MHz	PIFA antenna on mobile board (80×40×1.6) mm^3	PEC and silicon	(60×38×2.2) mm^3	Conductive and dielectric materials	40

Table 5. Comparison of SAR reduction by using SRR Metamaterials.

Reference	SAR source	Resonant frequency and BW	Antenna size	SRR type	SRRs size	Reduction on SAR (%)
[35] 2015	Traditional rectangle patch antenna	1.75 GHz	(49.6×59.6×1.6) mm^3	Traditional SRR superstrate	SRR radius of 20 mm built on (49.6×59.6×1.6) mm^3 substrate	86
[36] 2016	Circular monopole antenna	(2.1, 2.45 and 3.5) GHz, BW: 2.1 GHz	(30×30×0.8) mm^3	Partial SRR and pair of symmetrical stubs	Compactable with antenna in the same chip	12
[37] 2017	Mobile phone handset	(0.9, 1.8, 1.5 and 2.4) GHz, narrow BW	21.6 mm dipole, mobile board: (124×59×0.8) mm^3	Three integrated SRRs on a smart plastic case	Each SRR has diameter 15.2 mm and gab 0.8 mm	30
[38] 2018	Dipole antenna	0.9 GHz, BW: (0.5-3) GHz	(λ/2) dipole	Three traditional SRRs	(43.8×43.8×0.8) mm^3	84.3
[38] 2018	PIFA antenna	0.9 GHz, BW: (0.5-3) GHz	PIFA antenna built on (50×35×0.8) mm^3 substrate	One traditional SRR	(43.8×43.8×0.8) mm^3	23.7
[39] 2019	New design T-shaped planner antenna design	Multiple resonant (2.23, 2.4, 5, 5.8, 3, 3.5, 11.8 and 13.1) GHz	(0.26×0.253×0.0059) λ for frequency 2.23 GHz (35×34×0.8) mm^3	Slotted circular shape, and a complementary-SRR	Compactable with antenna in the same chip	13.3
[40] 2020	Mobile phone Model that exists on CST software	BW: (1.62-1.9) GHz, (2.08-2.21) GHz, (4.39-4.99) GHz, and (5.65-6.09) GHz	NA	(4×3) array SRRs and inversed E shaped structure resonator	Each SRR: (11.11×11.11×1.6) mm^3, SSRs array: (44.44×33.33×1.6) mm3	44

[41] 2021	Rectangular patch antenna, with two SRR	2.5 GHz and 5.5 GHz, BW: (2.2-2.6) GHz, (3.4-3.6) GHz, and (5-6.7) GHz	(20×13×1.6) mm^3	Metamaterial slab consists of an (5×3) array of pentagon split ring resonator	SSRs array built on (20×13×1.6) mm^3 substrate	84.5
[42] 2021	Mender line patch antenna	2.45 GHz, BW: 220MHz	(0.1856×0.2088×0.002946) λ	Hybrid SRR	The same antenna dimensions	0.651 W/Kg
[43] 2021	Mobile phone model that exists on CST software	(1.602, 2.712, and 3.88) GHz	NA	(2×3) hybrid SRR array	(24×36×0.3) mm^3	Up to 36.64

Table 6. Comparison of SAR reduction by using EBG.

Reference	SAR source	Resonant frequency and BW	Antenna size	EBG type	EBGs size	Reduction on SAR (%)
[53] 2015	Dipole antenna	Narrow bandwidth around 0.835 GHz	(λ/2) dipole	(4×6) EBG array chip	(51×35×3.4284) mm^3	97.92
[54] 2016	Square patch antenna	Narrow bandwidth around 2.4 GHz	Antenna:(52.27×57.75×1.8) mm^3, Antenna with EBG: (220×220×1.8) mm^3	Group of traditional EBG units (5×5)	Each unit: (44×44×1.8) mm^3	77.9
[55] 2017	Compact wearable antenna	Narrow bandwidth around 2.4 GHz	(30×20×0.7) mm^3	Novel design of miniaturized EBG	(46×46×0.7) mm^3	95
[56] 2018	Textile square patch antenna	2.4 GHz, BW: (2.27-2.49)	(70×60×3.5) mm^3	E-shape EBG array (3×3)	Each unit: (17.5×20×3.5) mm^3, array: (52.5×60×3.5) mm^3	48.99
[57] 2019	T-shaped folded dipole antenna	Narrow bandwidth around 2.4 GHz	(34×34×0.1) mm^3	Novel design of EBG chip	(74×37×0.1) mm^3	99
[58] 2020	Oval-shaped monopole antenna	2.45 GHz, BW: (1.8-3.2)	(55×59×0.1) mm^3	(3×3) EBG array chip	Each unit: (25.7×25.7×3) mm^3, array: (75.7×75.7×3) mm^3	99.5
[59] 2020	Innovative belt antenna	2.45 GHz, BW: (1.8-3.2)	(31×57×7.6) mm^3	Textile array (4×3) EBG ground plane	Each unit: (34×34×t) mm^3, array: (124×94×t) mm^3, t=cotton thickness	98.52
[60] 2021	CWSLMA	2.45 GHz, BW: (2.3-2.72)	Antenna:(34×18×1.6) mm^3, Antenna with EBG: (78×74×3.6) mm^3	(3×3) array of hexagonal-shaped EBG chip	(78×74×1) mm^3	More than 90
[61] 2021	monopole antenna	Narrow bandwidth around (2.4, 3.5, and 5.8) GHz	(45.3×34.1×1) mm^3	(2×2) rectangular EBG array with slots	(69×69×2) mm^3	More than 95
[62] 2021	Microstrip antenna	Narrow bandwidth around 26 GHz	(32.1×22×0.35) mm^3	(4×3) EBG array	Compactable with antenna in the same chip	More than 69.9

Table 7. Comparison of SAR reduction by using hybrid method.

Reference	SAR source	Resonant frequencies and BW	Antenna size	SAR reduction technique	technique size	SAR value
[65] 2018	CPW antenna	Narrow bandwidth around 2.4 GHz	(30×20×0.7) mm^3	EBG and FSS	(60×60×2.4) mm^3	Reduction by 95 %
[66] 2018	PIFA antenna	Two narrow bandwidths around 2.4 GHz and 5.8 GHz	(60×30×2) mm^3	Directive antenna with EBG	(83×83×2) mm^3	Reduction by 98.74 %
[67] 2020	E-slot antenna	Narrow bandwidth around 2.4 GHz	(30×20×0.7) mm^3	DGS and EBG	(60×60×2.4) mm^3	Reduction by 90 %
[68] 2020	Two compact monopoles	Narrow bandwidth around 2.4 GHz and 3.9 GHz	(50×52×1.5) mm^3	DGS and AMC	(60×60×1.5) mm^3	Reduction by 99.5 %
[69] 2021	planner textile antenna	BW: (6.5-35) GHz	(10×10×0.7) mm^3	DGS and SRR	(10×15×0.7) mm^3	Achieve SAR < 2 W/Kg
[70] 2021	S-shaped antenna	(2.4, 5.8, 9, 9.5) GHz	(0.2×0.24×0.08) λo	EBG and SRR	(0.48×0.48×0.08) λo	Achieve SAR < 0.944 W/Kg

Table 8. The comparison between a group of recent 4G and 5G antenna designs in terms of antenna characteristics and application.

Reference	Antenna type	Resonant frequency and BW	Antenna performance	Antenna size	Application
[7]	Traditional monopole antenna	0.9 GHz, BW: (0.85-2.2) GHz	Return loss improved by 53.7%	-NIL-	Police or military application
[81]	Phase array antenna	2 GHz	Efficiency improved by 6.8 dBi	Array of (λ/2) monopole	Wideband 5G antenna for Mobile handset antenna
[9]	Modified monopole antenna	1.8GHz, BW: (1.75-1.9) GHz	Suitable radiation pattern	(42×28×1.6) mm3	Mobile handset antenna operating at GSM1800 band
[10]	T-shaped antenna	2.1 GHz, BW: (2.4-2.5) GHz and (2.5-2.69) GHz	Efficiency (44.7-69.9) %	(30×40×1.6) mm^3	ISM2450 and 4G LTF bands used for wearable applications
[17]	Dipole antenna	900 MHz	-NIL-	Dipole with length 0.95λ/2	Mobile phone technology
[41]	Rectangular patch antenna	3.5 GHz, BW: (2.2–2.6) GHz, (3.40–3.60) GHz, and (5.0–6.9) GHz	gain improved by 30 %	(20 × 13 × 1.6) mm3	WLAN and WiMAX bands application
[49]	Dipole antenna	3.5 GHz	Efficiency improved from 82% to 91 %	Complex (35×51×4.5) mm^3	4G wireless communication system antenna
[60]	CWSLMA	2.45 GHz (2.3–2.72) GHz	Efficiency 90 %	(78 × 74 × 3.6) mm3	WBAN applications
[63]	Modified monopole antenna	3.5 GHz (3.3-3.5) GHz	efficiency Improved by 94.3 %	(43×83×7.5) mm^3	4G-mobile antenna
[64]	Compact microstrip antenna	1.8 GHz and 2.45 GHz, BW (1.71-1.80) GHz and (2.40-2.49) GHz	63 % impedance matching 28% miniaturization	(24.8×24.8×0.8) mm^3	GSM1800 and ISM2450 bands applications
[68]	Two compact monopole antennas	2.4 GHz and 3.9 GHz	Gain improved by 85 %	-NIL-	ISM and WiMAX bands

Table 9. The comparison between a group of recent 4G and 5G antenna designs in terms of SAR reduction.

Reference	human model used	Simulation Program	Separation distance (from the body)	Technique Used to reduce SAR	SAR Reduction (%)
[7]	-NIL-	-NIL-	(20-30) Cm	Reflector	
[81]	Lossy dielectric sphere modeled by FDTD	Numerical calculation, MoM/FDTD hybrid Methods	0.12 λ=18 mm	Phase array antenna as an antenna with reflector	(33-81.5) %
[9]	SAM phantom head model	CST microwave studio and ANSOFT HFSS software	(10-40) mm	Highly directive antenna (monopole)	20 %
[10]	-NIL-	ANSOFT HFSS and COMSOL software	(2-15) mm	Modified T-Shape antenna with AMC ground plane	25.19 %
[17]	Two-layer spherical shell	Computational software	5 mm	RF-shield of conductor (Nickel)	97.7 %
[41]	A cubical tissue model/ Human Head Model	-NIL-	8 mm	Polygonal SRR	84.50/55.72 %
[49]	Homogeneous cubic model comprised of musk	CST microwave studio software	10 mm	Dipole antenna above the EBG substrate	84 %
[60]	Three-layered cubic structure model	3D-electromagnetic simulator	-NIL-	3×3 EBG array	99 %
[63]	Homogenous cubic model/ anatomical human model	CST microwave studio Software/FDTD and the hybrid FEM/MoM Methods	-NIL-	Hybrid method EBG +Phase array as reflector	(70-90) %
[64]	A humane structure of log model as human tissue	ANSOFT HFSS software	-NIL-	Hybrid method Split ring resonator (SRR) + directive antenna	93 %
[68]	An artificial multi-layered human tissue model	-NIL-	5 mm	DGS+AMC	99.5 %

Table 10. The comparison between the proposed MIMO configurations and several recent related works.

Reference	SAR source (Antenna type)	Resonant frequencies and BW	No of elements	SAR reduction Technique	SAR reduction Technique size	MIMO system size	Peak SAR value
[22] 2021	Monopole antenna	BW: (2.075-2.625) GHz.	4	FSS and EBG	(120 × 120 × 1) mm^3	(50.5 × 38 × 1) mm^3	<0.2 W/Kg
[78] 2021	Monopole antenna	2.45 GHz, BW: 300 MHz	2	U-shaped and L-shaped DGS	Compactable with antenna in the same chip	(28×25×0.51) mm^3	<0.512 W/Kg
[79] 2021	Novel shape wearable patched antenna	BW: (4.5-6.5) GHz	4	Uniplanar compact EBG (UC-EBG)	Each unit: (10×10×1.15) mm^3, Array: (170×70×1.15) mm^3	(140×27.3×1.15) mm^3, separately from EBG array	<0.59 W/Kg
[80] 2021	Coupled folded antenna	3.2 GHz, BW: (3-5) GHz	6	Rectangular DGS array	Each unit: (4.5×4.5×0.8) mm^3	(134×75×0.8) mm^3	<2 W/Kg

References

[1] M. El Atrash, M. A. Abdalla, and H. M. Elhennawy, "A compact flexible textile artificial magnetic conductor-based wearable monopole antenna for low specific absorption rate wrist applications," International Journal of Microwave and Wireless Technologies, vol. 13, pp. 119-125, 2021.

[2] R. Seetharaman, M. Tharun, S. Gayathri, S. S. Mole, and K. Anandan, "Analysis of specific absorption rate and heat transfer in human head due to mobile phones," Materials Today: Proceedings, 2021.

[3] S. I. Al-Mously, "Factors influencing the EM interaction between mobile phone antennas and human head," in International Conference on Digital Information and Communication Technology and Its Applications, 2011, pp. 106-120.

[4] W. C. Choi, K. J. Kim, Y. J. Yoon, and J. U. Ha, "Inverted-F antenna with modified current distribution for SAR reduction," in 2014 International Workshop on Antenna Technology: Small Antennas, Novel EM Structures and Materials, and Applications (iWAT), 2014, pp. 36-39.

[5] N. Ramanpreet, M. Rattan, and S. S. Gill, "Compact and Low Profile Planar Antenna with Novel Metastructure for Wearable MBAN Devices," Wireless Personal Communications, pp. 1-13, 2021.

[6] M. Jung and B. Lee, "Evaluation of SAR reduction for mobile communication handsets," in IEEE Antennas and Propagation Society International Symposium (IEEE Cat. No. 02CH37313), 2002, pp. 444-447.

[7] M. Haridim, "Use of rod reflectors for SAR reduction in human head," IEEE Transactions on Electromagnetic Compatibility, vol. 58, pp. 40-46, 2015.

[8] N. T. Atanasov, G. L. Atanasova, A. K. Stefanov, and I. I. Nedialkov, "A wearable, low-profile, fractal monopole antenna integrated with a reflector for enhancing antenna performance and SAR reduction," in 2019 IEEE MTT-S International Microwave Workshop Series on Advanced Materials and Processes for RF and THz Applications (IMWS-AMP), 2019, pp. 67-69.

[9] D. Laila, R. Sujith, C. Nijas, C. Aanandan, K. Vasudevan, and P. Mohanan, "Modified CPW Fed Monopole Antenna with Suitable Radiation Pattern for Mobile Handset," Microwave review, 2011.

[10] S. Bhattacharjee, M. Mitra, and S. R. B. Chaudhuri, "An effective SAR reduction technique of a compact meander line antenna for wearable applications," Progress In Electromagnetics Research M, vol. 55, pp. 143-152, 2017.

[11] R. Pikale, D. Sangani, P. Chaturvedi, A. Soni, and M. Munde, "A review: methods to lower specific absorption rate for mobile phones," in 2018 International Conference On Advances in Communication and Computing Technology (ICACCT), 2018, pp. 340-343.

[12] J. P. Stephen and D. J. Hemanth, "An investigation on specific absorption rate reduction materials with human tissue cube for biomedical applications," International Journal of RF and Microwave Computer-Aided Engineering, vol. 29, p. e21960, 2019.

[13] P. Dhanesh, M. J. George, and B. Anoop, "A review on SAR reduction methods used for mobile application," IOSR Journal of Electronics and Communication Engineering (IOSR-JECE), vol. 10, pp. 25-27, 2015.

[14] L. H. Hemming, Architectural electromagnetic shielding handbook: a design and specification guide: John Wiley & Sons, 2000.

[15] K. Chan, K. Chow, L. Fung, and S. Leung, "Effects of using conductive materials for SAR reduction in mobile phones," Microwave and optical technology letters, vol. 44, pp. 140-144, 2005.

[16] N. H. M. Hanafi, M. T. Islam, N. Misran, and M. R. I. Faruque, "Numerical analysis of aluminium sheet for SAR reduction," in Proceeding of the 2011 IEEE International Conference on Space Science and Communication (IconSpace), 2011, pp. 281-285.

[17] R. B. Rani and S. Pandey, "Mobile phone radiation reduction using shield made of different materials," in 2015 13th International Conference on Electromagnetic Interference and Compatibility (INCEMIC), 2015, pp. 176-178.

[18] P. K. Dutta, P. V. Y. Jayasree, and V. S. S. N. S. Baba, "SAR reduction in the modelled human head for the mobile phone using different material shields," Human-centric Computing and Information Sciences, vol. 6, pp. 1-22, 2016.

[19] L. Ragha and M. Bhatia, "Evaluation of SAR reduction for mobile phone using RF shield," International Journal of Recent Trends in Engineering, vol. 2, p. 58, 2009.

[20] L. K. Ragha and M. S. Bhatia, "Evaluation of SAR reduction for dipole antenna using RF shield," in 2009 Second International Conference on Emerging Trends in Engineering & Technology, 2009, pp. 1075-1079.

[21] M. Hossain, M. Faruque, and M. Islam, "A New Design of Cell Phone Body for the SAR Reduction in the Human Head," Applied Computational Electromagnetics Society Journal, vol. 30, 2015.

[22] B. Sugumaran, R. Balasubramanian, and S. K. Palaniswamy, "Reduced specific absorption rate compact flexible monopole antenna system for smart wearable wireless communications," Engineering Science and Technology, an International Journal, vol. 24, pp. 682-693, 2021.

[23] R. S. Kshetrimayum, "A brief intro to metamaterials," IEEE potentials, vol. 23, pp. 44-46, 2004.

[24] R. A. Shelby, D. R. Smith, and S. Schultz, "Experimental verification of a negative index of refraction," science, vol. 292, pp. 77-79, 2001.

[25] S. Enoch, G. Tayeb, P. Sabouroux, N. Guérin, and P. Vincent, "A metamaterial for directive emission," Physical review letters, vol. 89, p. 213902, 2002.

[26] R. Yadav, S. Yadav, and S. Yadav, "SRR and R-CSRR Loaded Reconfigurable Antenna with Multiband Notch Characteristics," in Proceedings of International Conference on ICT for Sustainable Development, 2016, pp. 407-415.

[27] S. Ghadarghadr and H. Mosallaei, "Dispersion diagram characteristics of periodic array of dielectric and magnetic materials based spheres," IEEE transactions on Antennas and Propagation, vol. 57, pp. 149-160, 2009.

[28] F. Mesa, R. Rodríguez-Berral, and F. Medina, "On the computation of the dispersion diagram of symmetric one-dimensionally periodic structures," Symmetry, vol. 10, p. 307, 2018.

[29] Y. I. Abdulkarim, Ş. Dalgaç, F. O. Alkurt, F. F. Muhammadsharif, H. N. Awl, S. R. Saeed, et al., "Utilization of a triple hexagonal split ring resonator (SRR) based metamaterial sensor for the improved detection of fuel adulteration," Journal of Materials Science: Materials in Electronics, vol. 32, pp. 24258-24272, 2021.

[30] P. Gay-Balmaz and O. J. Martin, "Electromagnetic resonances in individual and coupled split-ring resonators," Journal of applied physics, vol. 92, pp. 2929-2936, 2002.

[31] R. Marques, J. Martel, F. Mesa, and F. Medina, "Left-handed-media simulation and transmission of EM waves in subwavelength split-ring-resonator-loaded metallic waveguides," Physical review letters, vol. 89, p. 183901, 2002.

[32] J. D. Baena, J. Bonache, F. Martín, R. M. Sillero, F. Falcone, T. Lopetegi, et al., "Equivalent-circuit models for split-ring resonators and complementary split-ring resonators coupled to planar transmission lines," IEEE transactions on microwave theory and techniques, vol. 53, pp. 1451-1461, 2005.

[33] J. B. Pendry, A. J. Holden, D. J. Robbins, and W. Stewart, "Magnetism from conductors and enhanced nonlinear phenomena," IEEE transactions on microwave theory and techniques, vol. 47, pp. 2075-2084, 1999.

[34] S. Harnsoongnoen, "Microwave sensors based on coplanar waveguide loaded with split ring resonators: A review," Applied Science and Engineering Progress, vol. 12, pp. 224-234, 2019.
[35] S. Imaculate Rosaline and S. Raghavan, "Design and analysis of a SRR superstrate for SAR reduction," Journal of Electromagnetic Waves and Applications, vol. 29, pp. 2330-2338, 2015.
[36] S. I. Rosaline and S. Raghavan, "Split ring loaded broadband monopole with SAR reduction," Microwave and Optical Technology Letters, vol. 58, pp. 158-162, 2016.
[37] H. Zhou, A. Pal, A. Mehta, and D. Mirshekar-Syahkal, "A smart mobile handset plastic case with integrated split ring resonators to reduce SAR," in 2017 IEEE International Symposium on Antennas and Propagation & USNC/URSI National Radio Science Meeting, 2017, pp. 1255-1256.
[38] H. Messaoudi and T. Aguili, "Use of a Split Ring Resonators with Dipole and PIFA Antenna to Reduce the SAR in a Spherical Multilayered Head Model," in 2018 6th International Conference on Multimedia Computing and Systems (ICMCS), 2018, pp. 1-6.
[39] R. K. Saraswat and M. Kumar, "A metamaterial hepta-band antenna for wireless applications with specific absorption rate reduction," International Journal of RF and Microwave Computer-Aided Engineering, vol. 29, p. e21824, 2019.
[40] A. M. Tamim, M. R. I. Faruque, E. Ahamed, and M. T. Islam, "Electromagnetic absorption of SRR based double-inverse E-Shaped metamaterial for DCS, EESC, 5G, and WiMAX applications," Chinese Journal of Physics, vol. 66, pp. 349-361, 2020.
[41] I. Rosaline, "A Triple-Band Antenna with a Metamaterial Slab for Gain Enhancement and Specific Absorption Rate (SAR) Reduction," Progress In Electromagnetics Research C, vol. 109, pp. 275-287, 2021.
[42] N. Ganeshwaran, J. Kailairajan Jeyaprakash, and G. N. A. Mohammed, "Compact coplanar waveguide fed implantable antenna with hybrid split-ring resonators," International Journal of RF and Microwave Computer-Aided Engineering, vol. 31, p. e22625, 2021.
[43] T. Ramachandran, M. R. I. Faruque, and M. T. Islam, "Dielectric passive left-handed symmetric metamaterial design for electromagnetic absorption reduction application," Proceedings of the Institution of Mechanical Engineers, Part L: Journal of Materials: Design and Applications, p. 1464420720985262, 2021.
[44] P. P. Bhavarthe, S. S. Rathod, and K. Reddy, "A compact dual band gap electromagnetic band gap structure," IEEE Transactions on Antennas and Propagation, vol. 67, pp. 596-600, 2018.
[45] B. Mohajer Iravani, "Electromagnetic interference reduction using electromagnetic bandgap structures in packages, enclosures, cavities, and antennas," 2007.
[46] F. Yang and Y. Rahmat-Samii, Electromagnetic band gap structures in antenna engineering: Cambridge university press Cambridge, UK, 2009.
[47] S. Chauhan and P. Singhal, "Comparative analysis of different types of planer EBG structures," International Journal of Scientific and Research Publications, vol. 4, pp. 1-5, 2014.
[48] N. Melouki, A. Hocini, and T. A. Denidni, "Performance enhancement of a compact patch antenna using an optimized EBG structure," Chinese Journal of Physics, vol. 69, pp. 219-229, 2021.
[49] R. Ikeuchi and A. Hirata, "Dipole antenna above EBG substrate for local SAR reduction," IEEE Antennas and Wireless Propagation Letters, vol. 10, pp. 904-906, 2011.
[50] A. Khan, S. Bashir, and F. Ullah, "Electromagnetic bandgap wearable dipole antenna with low specific absorption rate," in 2018 International Conference on Computing, Mathematics and Engineering Technologies (iCoMET), 2018, pp. 1-4.
[51] U. Ali, S. Ullah, M. Shafi, S. A. Shah, I. A. Shah, and J. A. Flint, "Design and comparative analysis of conventional and metamaterial-based textile antennas for wearable applications," International Journal of Numerical Modelling: Electronic Networks, Devices and Fields, vol. 32, p. e2567, 2019.
[52] M. Beruete, M. Sorolla, R. Marqués, J. Baena, and M. Freire, "Resonance and cross-polarization effects in conventional and complementary split ring resonator periodic screens," Electromagnetics, vol. 26, pp. 247-260, 2006.
[53] A. Tharakan, J. Deepthi, D. A. Sebastian, J. Gopika, and D. Krishna, "Specific absorption rate reduced (SAR) mobile phone antenna designs," in 2015 Fifth International Conference on Advances in Computing and Communications (ICACC), 2015, pp. 250-253.
[54] S. M. Umar, F. Ahmad, W. U. R. Khan, and S. Ullah, "Specific absorption rate analysis of a WLAN antenna using mushroom-type electromagnetic bandgap (EBG) structure," in 2016 13th International Bhurban Conference on Applied Sciences and Technology (IBCAST), 2016, pp. 631-635.
[55] A. Y. Ashyap, Z. Z. Abidin, S. H. Dahlan, H. A. Majid, S. M. Shah, M. R. Kamarudin, et al., "Compact and low-profile textile EBG-based antenna for wearable medical applications," IEEE Antennas and Wireless Propagation Letters, vol. 16, pp. 2550-2553, 2017.
[56] R. Manikonda, R. L. Valluri, and M. R. Prudhivi, "Specific absorption rate reduction using EBG structure as superstrate for textile antenna," ARPN Journal of Engineering and Applied Sciences, vol. 13, pp. 3495-3501, 2018.
[57] S. A. Balakrishnan and E. F. Sundarsingh, "Conformal self-balanced EBG integrated printed folded dipole antenna for wireless body area networks," IET Microwaves, Antennas & Propagation, vol. 13, pp. 2480-2485, 2019.
[58] M. El Atrash, O. F. Abdalgalil, I. S. Mahmoud, M. A. Abdalla, and S. R. Zahran, "Wearable high gain low SAR antenna loaded with backed all-textile EBG for WBAN applications," IET Microwaves, Antennas & Propagation, vol. 14, pp. 791-799, 2020.
[59] R. Pei, M. P. Leach, E. G. Lim, Z. Wang, C. Song, J. Wang, et al., "Wearable EBG-backed belt antenna for smart on-body applications," IEEE Transactions on Industrial Informatics, vol. 16, pp. 7177-7189, 2020.
[60] S. Singh and S. Verma, "SAR reduction and gain enhancement of compact wideband stub loaded monopole antenna backed with electromagnetic band gap array," International Journal of RF and Microwave Computer-Aided Engineering, p. e22813, 2021.
[61] W. El May, I. Sfar, J. M. Ribero, and L. Osman, "Design of Low-Profile and Safe Low SAR Tri-Band Textile EBG-Based Antenna for IoT Applications," Progress In Electromagnetics Research Letters, vol. 98, pp. 85-94, 2021.
[62] E. Wissem, I. Sfar, L. Osman, and J. Ribero, "A Textile EBG-Based Antenna for Future 5G-IoT Millimeter-Wave Applications. Electronics 2021, 10, 154," ed: s Note: MDPI stays neu-tral with regard to jurisdictional clai-ms in …, 2021.
[63] K.-H. Chan, R. Ikeuchi, and A. Hirata, "Effects of phase difference in dipole phased-array antenna above EBG substrates on SAR," IEEE Antennas and Wireless Propagation Letters, vol. 12, pp. 579-582, 2013.
[64] S. I. Rosaline and S. Raghavan, "A compact dual band antenna with an ENG SRR cover for SAR reduction," Microwave and Optical Technology Letters, vol. 57, pp. 741-747, 2015.
[65] A. Y. Ashyap, Z. Z. Abidin, S. H. Dahlan, H. A. Majid, M. R. Kamarudin, A. Alomainy, et al., "Highly efficient wearable CPW antenna enabled by EBG-FSS structure for medical body area network applications," IEEE Access, vol. 6, pp. 77529-77541, 2018.
[66] G. Gao, B. Hu, S. Wang, and C. Yang, "Wearable planar inverted-F antenna with stable characteristic and low specific

absorption rate," Microwave and Optical Technology Letters, vol. 60, pp. 876-882, 2018.
[67] A. Y. Ashyap, S. H. B. Dahlan, Z. Z. Abidin, M. H. Dahri, H. A. Majid, M. R. Kamarudin, et al., "Robust and efficient integrated antenna with EBG-DGS enabled wide bandwidth for wearable medical device applications," IEEE Access, vol. 8, pp. 56346-56358, 2020.
[68] B. Hazarika, B. Basu, and A. Nandi, "Design of antennas using artificial magnetic conductor layer to improve gain, flexibility, and specific absorption rate," Microwave and Optical Technology Letters, vol. 62, pp. 3928-3935, 2020.
[69] A. R. Alhawari, A. Almawgani, A. T. Hindi, H. Alghamdi, and T. Saeidi, "Metamaterial-based wearable flexible elliptical UWB antenna for WBAN and breast imaging applications," AIP Advances, vol. 11, p. 015128, 2021.
[70] K. K. Rao, "Design and Analysis of Metamaterial based-check board AMC Backed EBG Antenna for Body Placement Applications," INFORMATION TECHNOLOGY IN INDUSTRY, vol. 9, pp. 707-721, 2021.
[71] F. A. Dicandia and S. Genovesi, "Exploitation of triangular lattice arrays for improved spectral efficiency in massive MIMO 5G systems," IEEE Access, vol. 9, pp. 17530-17543, 2021.
[72] C.-Y.-D. Sim, H.-Y. Liu, and C.-J. Huang, "Wideband MIMO antenna array design for future mobile devices operating in the 5G NR frequency bands n77/n78/n79 and LTE band 46," IEEE Antennas and Wireless Propagation Letters, vol. 19, pp. 74-78, 2020.
[73] P. Garg and P. Jain, "Isolation improvement of MIMO antenna using a novel flower shaped metamaterial absorber at 5.5 GHz WiMAX band," IEEE Transactions on Circuits and Systems II: Express Briefs, vol. 67, pp. 675-679, 2019.
[74] Y. H. Lin and Y. S. Chen, "Reduction of multiple-input multiple-output specific absorption rate synthesized using a fast estimation model," International Journal of RF and Microwave Computer-Aided Engineering, vol. 29, p. e21961, 2019.
[75] D. T. T. Tu, N. T. B. Phuong, P. D. Son, and V. Van Yem, "Improving Characteristics of 28/38GHz MIMO Antenna for 5G Applications by Using Double-Side EBG Structure," J. Commun., vol. 14, pp. 1-8, 2019.
[76] W. Jiang, Y. Cui, B. Liu, W. Hu, and Y. Xi, "A dual-band MIMO antenna with enhanced isolation for 5G smartphone applications," IEEE Access, vol. 7, pp. 112554-112563, 2019.
[77] D. Serghiou, M. Khalily, V. Singh, A. Araghi, and R. Tafazolli, "Sub-6 GHz dual-band 8× 8 MIMO antenna for 5G smartphones," IEEE Antennas and Wireless Propagation Letters, vol. 19, pp. 1546-1550, 2020.
[78] A. Gupta, A. Kansal, and P. Chawla, "Design of a wearable MIMO antenna deployed with an inverted U-shaped ground stub for diversity performance enhancement," International Journal of Microwave and Wireless Technologies, vol. 13, pp. 76-86, 2021.
[79] H. Zu, B. Wu, P. Yang, W. Li, and J. Liu, "Wideband and High-Gain Wearable Antenna Array with Specific Absorption Rate Suppression," Electronics, vol. 10, p. 2056, 2021.
[80] A. M. Hediya, A. M. Attiya, and W. S. El-Deeb, "Multiple-Input Multiple-Output Antenna for Sub-Six GHz 5G Applications Using Coupled Folded Antenna with Defective Ground Surface," Progress In Electromagnetics Research C, vol. 114, pp. 13-29, 2021.
[81] M. Mangoud, R. Abd-Alhameed, N. McEwan, P. Excell, and E. Abdulmula, "SAR reduction for handset with two-element phased array antenna computed using hybrid MoM/FDTD technique," Electronics Letters, vol. 35, pp. 1693-1694, 1999.